Check for updates
Europe
European Chemical
Societies Publishing

Metallocenes

Rhodocenium Monocarboxylic Acid Hexafluoridophosphate and Its Derivatives: Synthesis, Spectroscopy, Structure, and Electrochemistry

Markus Jochriem,[a] Larissa A. Casper,[b] Stefan Vanicek,[a,c] Dirk Petersen,[c] Holger Kopacka,[a] Klaus Wurst,[a] Thomas Müller,[d] Rainer F. Winter,*[b] and Benno Bildstein*[a]

Abstract: As an extension of our continuing work in metallocenium chemistry, we report here on new functionalized rhodocenium salts. In contrast to isoelectronic cobaltocenium compounds, rhodium as a 4d metal allows synthetic routes via prefunctionalized cyclopentadienyl half-sandwich precursors, thereby facilitating access to monofunctionalized rhodocenium salts containing substituents comprising methyl, trimethylsilyl, carboxylate and carboxylate ester as well as amide derivatives. Synthetic aspects, scope and limitations, as well as spectroscopic (^{1}H/^{13}C-NMR, IR, HR-MS), and structural (XRD) properties are reported. Like the parent rhodocenium ion, all new derivatives undergo two chemically consecutive reductions at potentials that depend on the respective ring substituent. The second reduction competes with a rapid reaction of the corresponding rhodocenes to their 18 VE dimers. Rate constants for this process range from 2×10^3 s^{-1} to 2.5×10^5 s^{-1} as estimated from digital simulations of experimental voltammograms. Rhodocenium carboxylic acid (**8**) constitutes a special case in that proton instead of metal reduction is observed at Pt or Au electrodes.

Introduction

After almost 70 years of research in metallocene chemistry, still relatively little is known about cobaltocenium, rhodocenium and iridocenium salts that are isoelectronic and as stable and redox responsive as their ubiquitous ferrocene congeners. The main reason for the underdeveloped chemistry of these metallocenium salts is their intrinsic cationic nature, making it quite difficult to access functionalized derivatives by standard chemical reactions developed for arenes. However, in recent years

[a] *Institute of General, Inorganic and Theoretical Chemistry, University of Innsbruck, Center for Chemistry and Biomedicine, Innrain 80-82, 6020 Innsbruck, Austria*
E-mail: benno.bildstein@uibk.ac.at
https://www.uibk.ac.at/aatc/
[b] *Department of Chemistry, University of Konstanz, Universitätsstrasse 10, 784557 Konstanz, Germany*
E-mail: rainer.winter@uni-konstanz.de
https://www.chemie.uni-konstanz.de/winter/
[c] *Department of Chemistry, University of Oslo, Sem Sælands vei 26, 0315, Oslo Norway*
[d] *Institute of Organic Chemistry, University of Innsbruck, Center for Chemistry and Biomedicine, Innrain 80-82 6020 Innsbruck, Austria*

we were able to introduce valuable new synthetic protocols in cobaltocenium chemistry[1] that are currently used to access chemically interesting cobaltocenium compounds.[2] Our motivation for studying cobaltocenium compounds in general stems from their unique combination of advantageous properties like air-stability, reversible redox chemistry, high polarity with concomitant high solubility in polar solvents, and a strongly electron-withdrawing character, thereby opening up new applications in redox catalysis, bioinorganic chemistry, ligand design and coordination chemistry.[2]

In comparison to cobaltocenium chemistry, rhodocenium chemistry is even less developed.[3] In fact, only three monosubstituted rhodocenium compounds are presently known. First, Sheats and co-workers[4] reported in 1983 the synthesis of rhodocenium monocarboxylic acid hexafluoridophosphate in 20 % isolated yield by a non-chemoselective statistical approach, taking advantage of the differences in solubility of unsubstituted rhodocenium, rhodocenium mono- and rhodocenium dicarboxylic acid salts. No further chemistry of rhodocenium monocarboxylic acid hexafluoridophosphate was described. Second, Andre and co-workers[5] published in 1990 the preparative HPLC separation of ferrocenylrhodocenium from other metallocenylrhodocenium salts. The latter were again obtained by a statistical protocol. Third, Yan and co-workers[6] reported in 2015 a hydroxyethyltriazolylrhodocenium salt obtained from (η^4-ethynylcyclopentadiene)(η^5-cyclopentadienyl)rhodium(I) by azide-alkyne cycloaddition followed by oxidation with ferrocenium hexafluoridophosphate. This rhodocenium-functionalized alcohol was converted to norbornene and methacrylate mono-

EurJIC
European Journal of Inorganic Chemistry

Full Paper
doi.org/10.1002/ejic.202000071

Chemistry
Europe
European Chemical
Societies Publishing

mers and subsequently polymerized to the corresponding side-chain functionalized redox-responsive polymers.

In this contribution, we aim at developing rhodocenium chemistry a bit further, in part based on our experience in cobaltocenium chemistry,[1,2] and disclose here a first chemoselective synthesis of rhodocenium monocarboxylic acid hexafluoridophosphate which is a key synthon for other monosubstituted rhodocenium salts accessible by standard carboxylic acid reactivity. The structural, spectroscopic and electrochemical properties of these new rhodocenium derivatives are compared with those of their cobaltocenium congeners.
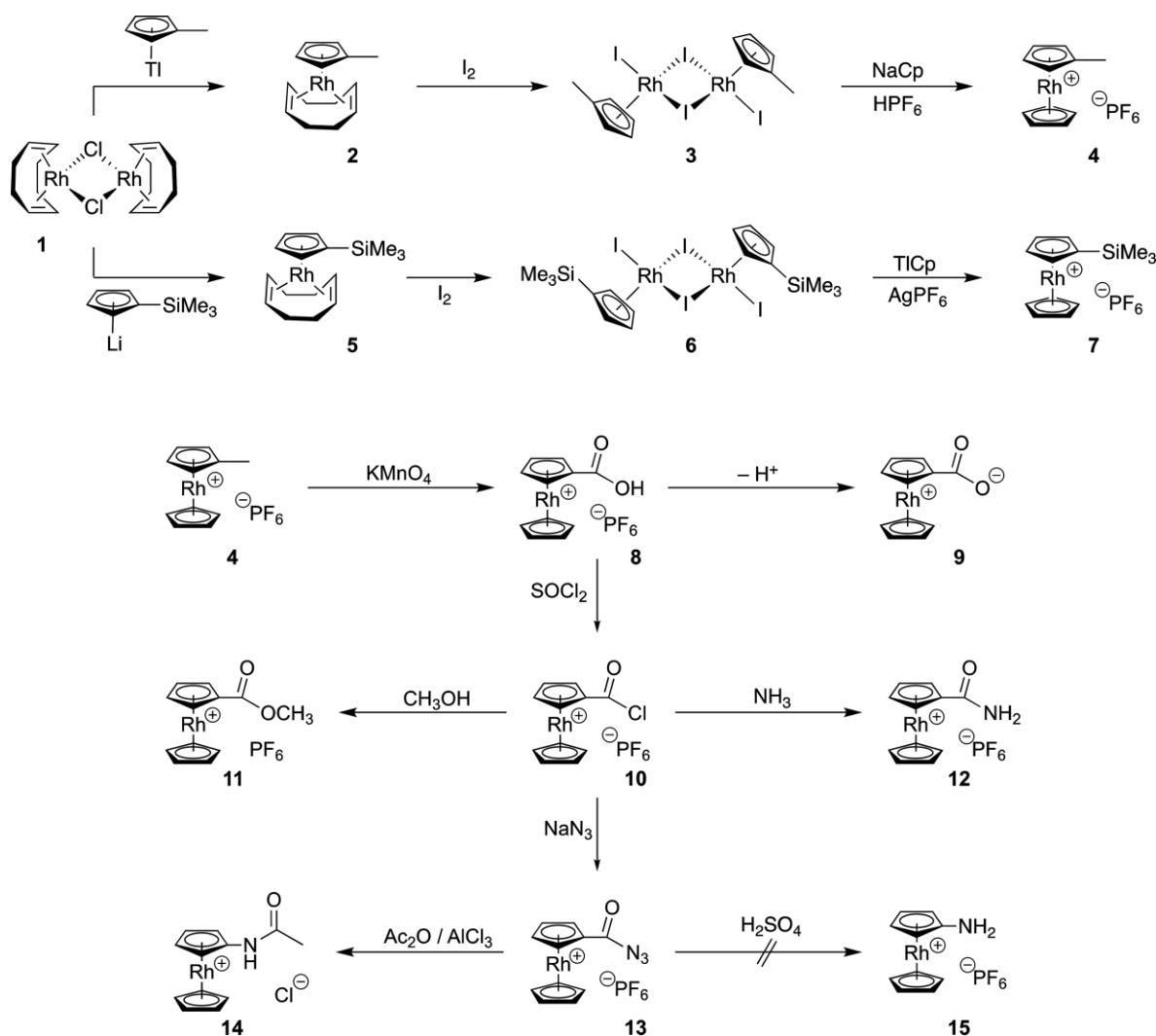
Results and Discussion

Synthesis

In general, rhodocenium chemistry is somewhat different from cobaltocenium chemistry, as is often observed when comparing the reactivities and stabilities of analogous compounds of 3d vs. 4d/5d metals in a homologous group of elements. Successful synthetic routes to cobaltocenium compounds cannot simply

be applied for rhodocenium compounds, due to differences in either reactivity or solubility of cobaltocenium/rhodocenium salts. Specifically, while the main target of this study, rhodocenium monocarboxylic acid hexafluoridophosphate, could be generated by a nucleophilic addition/hydride removal/side-chain oxidation sequence that was recently developed in our group for the successful synthesis of its cobaltocenium analogue,[1a] its purification from side products and isolation proved not feasible despite many efforts. Similarly, direct amination of rhodocenium salts by a vicarious nucleophilic substitution gave only inseparable product mixtures, in contrast to corresponding cobaltocenium salts.[1c] Therefore alternative synthetic strategies are needed for new monofunctionalized rhodocenium compounds. In this context, an advantageous feature of rhodium chemistry is the much higher stability of half-sandwich rhodium(III) halide complexes[7] in comparison to their labile cobalt(III) analogues.[8] As we will see in the following, these rhodium(III) species are valuable synthons for our purposes (Scheme 1).

Freshly prepared thallium methylcyclopentadienide (Cp'Tl) was reacted in dry tetrahydrofuran under an atmosphere of ar-

Scheme 1. Synthesis of compounds.

EurJIC
European Journal of Inorganic Chemistry

Full Paper
doi.org/10.1002/ejic.202000071

**Chemistry
Europe**
European Chemical
Societies Publishing

gon with chlorido(cyclooctadiene)rhodium(I) dimer (**1**) to afford (cyclooctadiene)(methylcyclopentadienyl)Rh(I) (**2**) as an air-stable yellow oil. Without further purification, oxidation of **2** with diiodine gave di(methylcyclopentadienyl)-dirhodium(III) tetraiodide (**3**) in a satisfactory overall yield of 67 %. Reaction of **3** with two equivalents of sodium cyclopentadienide (NaCp) followed by precipitation of the product with aqueous hexafluorophosphoric acid afforded methylrhodocenium hexafluoridophosphate (**4**) in 77 % isolated yield as an air-stable white powder. In a similar manner, trimethylsilylrhodocenium hexafluoridophosphate (**7**) was obtained from **1** by treatment with lithium trimethylsilylcyclopentadenide via the silylated Rh(I)/Rh(III) complexes **5/6** in 66 % overall yield. Starting from lithium trimethylstannylcyclopentadienide, an analogous reaction sequence was performed aiming at trimethylstannylrhodocenium hexafluoridophosphate, a potentially useful synthon for Stille cross-coupling reactions. However, due to the weaker carbon–tin bond, undesired redox processes prevented a successful reaction.

Methylrhodocenium hexafluoridophosphate (**4**) served in the following as precursor for further monosubstituted rhodocenium salts. In analogy to early work by Sheats and co-workers,[4] aromatic side-chain oxidation of **4** with basic potassium permanganate afforded white rhodocenium-monocarboxylic acid hexafluoridophosphate (**8**) in 90 % isolated yield. Being an unusual cationic carboxylic acid, **8** could be deprotonated on an anion-exchange resin to provide the zwitterionic rhodocenium carboxylate (**9**). **9** constitutes an interesting new neutral

carboxylato ligand, similar to its analogous cobalt congener.[2d] Derivatives of monocarboxylic acid hexafluoridophosphate (**8**) were synthesized by standard organic transformations. Quantitative conversion of **8** to rhodoceniumcarboxylic acid chloride hexafluoridophosphate (**10**) was performed in refluxing thionyl chloride, followed by esterification with methanol to methoxycarbonylrhodocenium hexafluoridophosphate (**11**) or amide formation with aqueous ammonia to rhodoceniumcarboxylic acid amide hexafluoridophosphate (**12**), respectively. A major target compound of this work was aminorhodocenium hexafluoridophosphate (**15**), due to the high synthetic potential of the amino functionality. In analogy to cobaltocenium chemistry,[1b,4] the azide derivative **13** was prepared from **10** with sodium azide. Conversion of compound **13** to **15** in refluxing concentrated sulfuric acid by classic Curtius rearrangement worked out in part according to NMR analysis of the crude product mixture, but despite all our efforts at optimization, separation of the product mixture and isolation of pure **15** proved so far impossible. For "difficult" organic substrates, a modified Lewis acid-assisted Curtius rearrangement[9] to acyl-protected amines followed by solvolysis to the free amino derivative was developed. By applying this methodology, acetamidorhodocenium chloride (**14**) was synthesized in 60 % yield, but unfortunately its acidic or basic hydrolysis to the desired aminorhodocenium hexafluoridophosphate (**15**) met so far only with limited success (appr. 40 % conversion according to NMR analysis) and no methods to isolate **15** from these reaction mixtures proved possible.
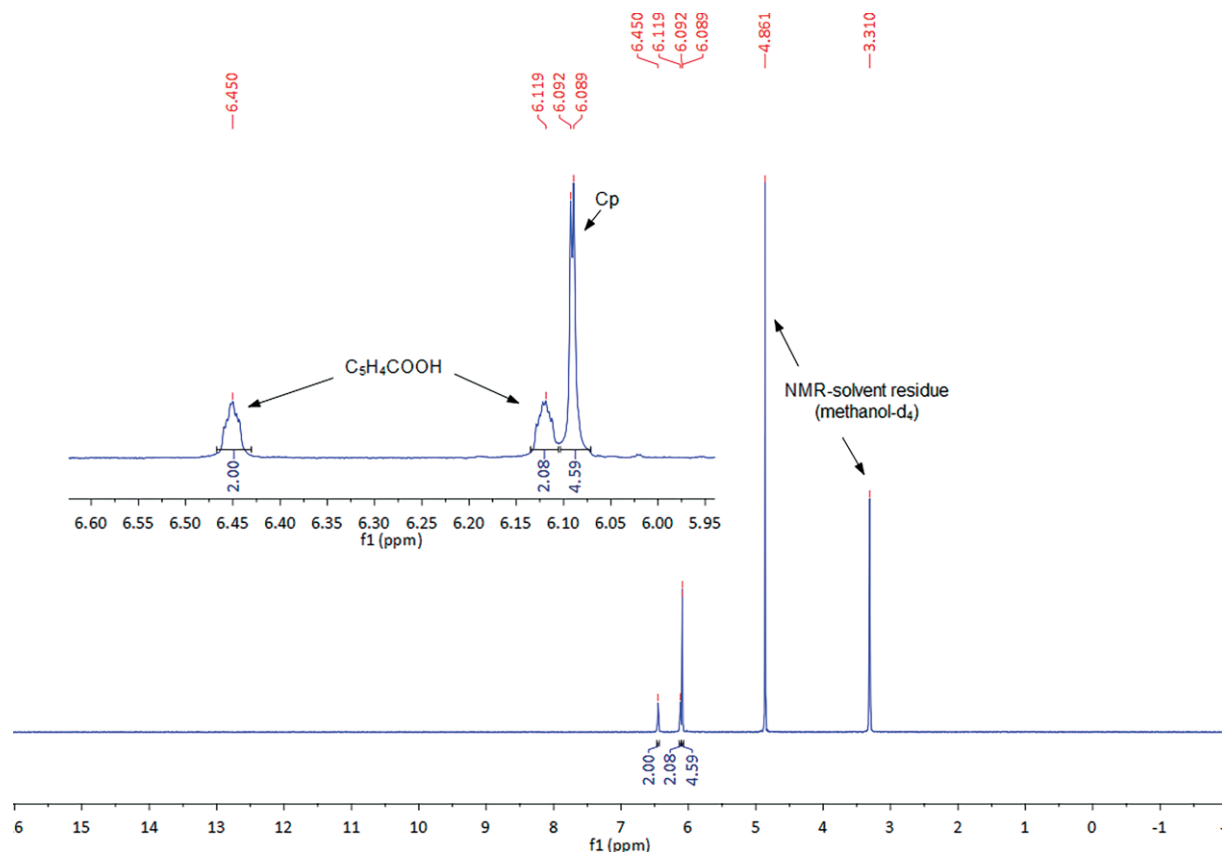

Figure 1. ^{1}H-NMR spectrum of rhodoceniumcarboxylic acid hexafluoridophosphate (**8**) in [D$_4$]methanol solution.

EurJIC
European Journal of Inorganic Chemistry

Full Paper
doi.org/10.1002/ejic.202000071

Chemistry
Europe
European Chemical
Societies Publishing

Physical, Spectroscopic, and Structural Properties

Rhodocenium salts **4**, **7**, **8**, **11**, **12**, and **14** are highly stable with melting points in the range of 173°-280° C whereas **9**, **10** and **13** are hydrolytically unstable. In general, rhodocenium salts are less colored than their usually yellow to orange cobalt analogues,[1,2] due to stronger metal-ligand bonding of 4d elements. Rhodocenium salts are highly polar compounds, soluble in polar solvents like acetonitrile, dimethyl sulfoxide, methanol, acetone and water, an advantageous property for potential applications in green chemistry or for bioorganometallic chemistry. Hexafluoridophosphate is the most convenient and preferred counterion, allowing precipitation of products from aqueous solutions in the workup procedure. Spectroscopically, the hexafluoridophosphate ion was easily identified by its strong IR absorptions at $\approx$ 820 and 550 cm^{-1}. In addition, diagnostic IR signals for the functional groups of rhodocenium salts **8–14** were observed (compare experimental section and spectra in the Supporting Information). High resolution mass spectrometry gave signals of the cations in excellent agreement with theoretical values. ^{1}H- and ^{13}C-NMR spectroscopy allowed for structural characterization of these monosubstituted rhodocenium compounds in solution. ^{1}H-NMR spectra showed in the region of 5.8–6.5 ppm the common pattern of monosubstituted metallocenes (1 signal corresponding to 5H, two pseudotriplets corresponding to 2H) with additional two-bond scalar couplings [$^2J(^1$H-^{103}Rh) $\approx$ 1 Hz] to ^{103}Rh, a 100 % naturally abundant spin 1/2 nucleus (see Experimental Section and spectra in the Supporting Information). Additional appropriate resonances were observed for the respective substituents. Figure 1 shows the ^{1}H-NMR spectrum of rhodoceniumcarboxylic acid hexafluoridophosphate (**8**) as a representative example.

In the ^{13}C-NMR spectra of rhodocenium salts the signals of the carbon atoms of the Cp ligands were observed in the region of 85–95 ppm as doublets with $^1J(^{13}$C-^{103}Rh) $\approx$ 7 Hz, together with ^{103}Rh-uncoupled signals of the carbon atoms due to the respective functional group (see Experimental Section and spectra in the Supporting Information).

In general, characterization of rhodium compounds by ^{103}Rh-NMR spectroscopy[10] is rarely done, simply because most NMR spectrometers are not adequately equipped for ^{103}Rh measurements. Although the element rhodium has a ^{103}Rh nucleus of spin of 1/2 with 100 % natural abundance, direct observation of ^{103}Rh signals is quite difficult due to the extremely low gyromagnetic ratio (γ = –0.8420×10^7 radT^{-1} s^{-1}), the low receptivity ($\approx$ 0.2 % of that of ^{13}C), and the extremely large chemical shift range ($\approx$ 13000 ppm). However, diamagnetic Rh(I) or Rh(III) compounds with scalar couplings to other nuclei (^{1}H, ^{13}C, ^{31}P) allow for application of magnetization transfer pulse sequences like INEPT (insensitive nuclei enhanced by polarization transfer) that increase the sensitivity to approximately 20 % of that of ^{13}C. Rhodocenium salts **4**, **7**, **8**, **11**, **12**, and **14** with their heteronuclear coupling to ^{1}H and ^{13}C [$^2J(^1$H-^{103}Rh) $\approx$ 1 Hz, $^1J(^{13}$C-^{103}Rh) $\approx$ 7 Hz] are therefore good candidates for such measurements. However, whereas detection of the corresponding signal for the unsubstituted parent compound rhodocenium hexafluoridophosphate, Cp$_2$Rh$^+$PF$_6^-$, proved possible (δ = –10122.80 ppm vs. Rh(acac)$_3$), repeated

attempts on substituted rhodocenium salts **4**, **7**, **8**, **11**, **12**, and **14** met so far without conclusive results, even when applying carefully optimized spectrometer settings.

Single crystal structures are available for compounds **3**, **7**, **8**, **11**, **12** and **14** (Figure 2, Figure 3, Figure 4, Figure 5, Figure 6,
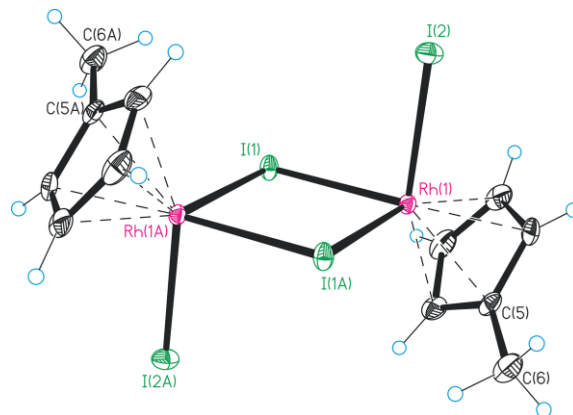

Figure 2. Molecular structure of **3** with thermal ellipsoids at a 50 % probability. Selected bond lengths [Å] and angles (°): Rh(1)–I(1) = 2.7001(3), Rh(1)–I(2) = 2.6817(3); Rh(1)–I(1)–I(1A) = 94.402(8), I(1)–Rh(1)–I(2) = 92.024(9), I(2)–Rh(1)–I(1A) = 91.976(9), I(1)–Rh(1)–I(1A) = 85.598(8).

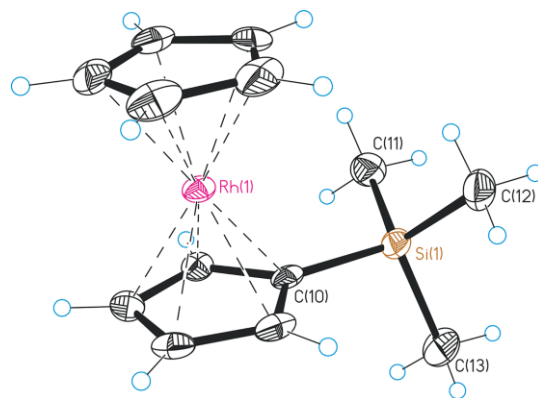Figure 3. Molecular structure of **7** with thermal ellipsoids at a 50 % probability, counterions PF$_6$ (65 % occupancy) and I (35 % occupancy) omitted for clarity. Selected bond length [Å] C(10)–Si(1) = 1.876(5).
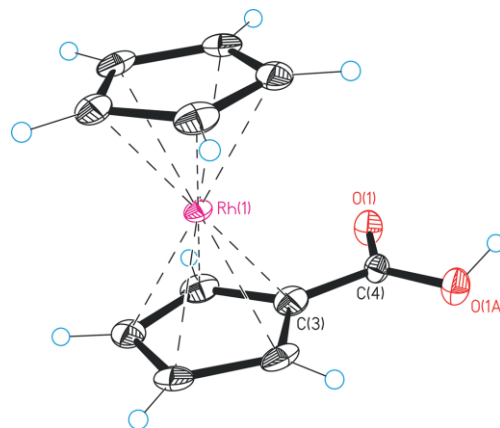

Figure 4. Molecular structure of **8** with thermal ellipsoids at a 50 % probability, counterion PF$_6$ omitted for clarity. Selected bond lengths [Å]: C(3)–C(4) = 1.403(7), C(4)–O(1) = C(4)–O(1A) = 1.258(4).

EurJIC
European Journal of Inorganic Chemistry

Full Paper
doi.org/10.1002/ejic.202000071

Chemistry Europe
European Chemical Societies Publishing

and Figure 7). Rhodium(III) halide precursor **3** shows the expected dimeric structure with bridging and terminal iodide ligands, similar as in derivatives with cyclopentadienyl ligands other than Cp′.[7] Rhodocenium salts **7**, **8**, **11** and **12** display
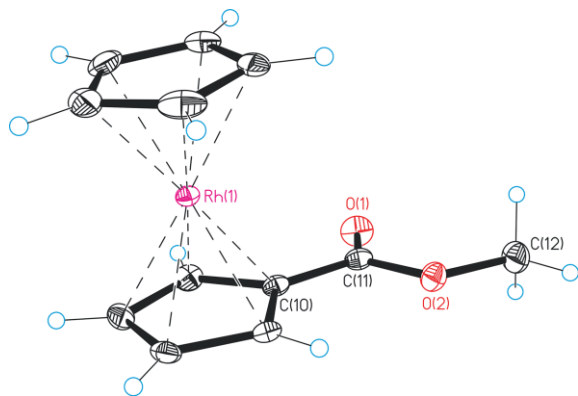

Figure 5. Molecular structure of **11** with thermal ellipsoids at a 50 % probability, counterion PF_6 omitted for clarity. Selected bond lengths [Å]: C(10)–C(11) = 1.480(3), C(11)–O(1) = 1.201(2), C(11)–O(2) = 1.327(2), O(2)–C(12) = 1.449(2).
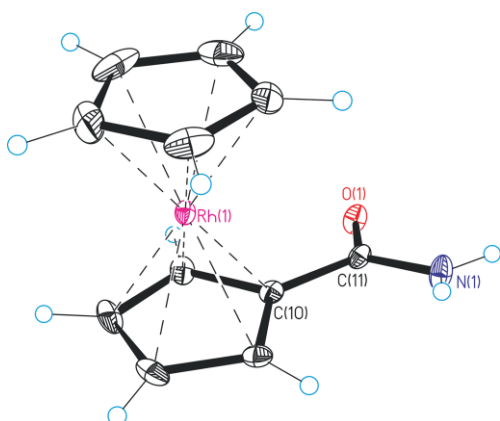

Figure 6. Molecular structure of **12** with thermal ellipsoids at a 50 % probability, counterion PF_6 omitted for clarity. Selected bond lengths [Å] and angles (°): C(10)–C(11) = 1.431(4), C(11)–O(1) = 1.226(4), C(11)–N(1) = 1.335(4).
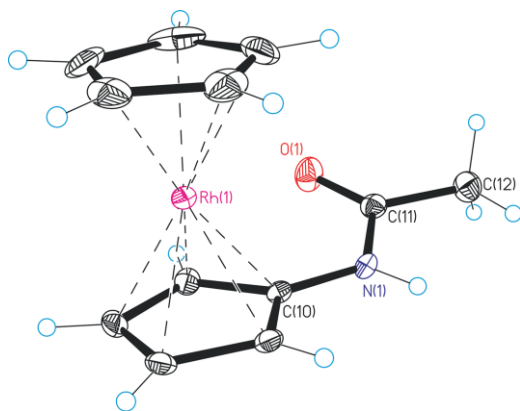

Figure 7. Molecular structure of **14** with thermal ellipsoids at a 50 % probability, counterion Cl and H_2O solvent molecule omitted for clarity. Selected bond lengths [Å] and angles (°): C(10)–N(1) = 1.388(4), N(1)–C(11) = 1.365(4), C(11)–O(1) = 1.219(3), C(11)–C(12) = 1.499(4).

overall regular, undistorted metallocene moieties with rhodium–carbon bond lengths in the range of 2.147 to 2.188 Å (see Supporting Information). In the structure of **14**, the bond length of Rh to the substituted carbon atom is slightly elongated [Rh(1)–C(10) = 2.201(3) Å] with a slightly shortened C(10)–N(1) bond of 1.388(4) Å. This indicates some contributions of an imine fulvenoid resonance structure, a common feature of *N*-substituted metallocenium salts.[1b] In the structure of **8**, hydrogen-bonded dimers of the carboxylic functionality are observed with anti-oriented rhodocenium moieties (see Supporting Information), quite analogous to the structure of cobaltocenium carboxylic acid hexafluoridophosphate.[1a]

Electrochemistry

The electrochemical properties of the parent rhodocenium ion and of several ring-substituted derivatives have been studied on several occasions. Neutral rhodocenes generally lack the chemical stability of their lighter cobaltocene homologues in agreement with the much higher propensity of complexes of 4d and 5d metal ions to obey the 18 valence electron rule. Parent rhodocene, generated by the chemical or electrochemical reduction of the rhodocenium ion, has a half-life of only about 2 seconds at r. t.[11] It rapidly evolves into a stable dihydrofulvalene-bridged dimer $[\{(\eta^5\text{-}C_5H_5)Rh\}_2(\mu,\eta^4{:}\eta^4\text{-}C_{10}H_{10})]$, where the bridging bis(diene)-type ligand donates four electrons to every rhodium atom such that the Rh atoms maintain their 18 VE count (Scheme 2). Further reduction of unstable rhodocene to the associated, even more reactive anion can nevertheless be observed as a chemically irreversible process and occurs at a ca. 770 mV lower (more negative) potential (Table 1). Ring substitution at one or both cyclopentadienyl ligands exerts a strong influence on the reduction potentials of the +/0 and 0/– processes and the chemical stabilities of the reduced formally 19 or 20 valence electron rhodocenes or rhodocene anions. Permethylation of one Cp ligand as in [Cp*CpRh]+ (Cp* = pentamethylcyclopentadienyl) shifts the two consecutive reductions by 260 mV or 480 mV to more negative potentials but fails to stabilize the corresponding rhodocene against dimerization; instead an unsymmetrical dimer with a new C–C bond between a former Cp and Cp* ligand results.[12] Methylation of the second Cp ring as in [Cp*₂Rh]+ or [Cp*Cp^Me4Rh]+ (Cp^Me4 = η^5-tetramethlycyclopentadienide) decreases the reduction potential further but, while preventing dimerization, still fails to chemically stabilize the corresponding neutral rhodocenes against other follow-reactions.[12,13] Higher stabilities of reduced rhodocenium ions were reported for congeners with the Cp‴ (Cp‴ = 1,2,3-tri^tert^butylcyclopentadienide) ligand, culminating in the observation of two chemically reversible reductions of the [Cp‴Cp*Rh]+ cation.[14] Again, sizeable cathodic shifts of the reduction potentials on replacing the Cp ligand by Cp* were noted (Table 1). The only stable rhodocenes with a genuine sandwich structure reported to date seem to be $[(\eta^5\text{-}C_5Ph_4H)_2Rh]$,[15] which could even be crystallized and investigated by X-ray crystallography, and [Cp*(η^5-indenyl)Rh].[12] In the former complex, the bulky C_5Ph_4H ligand prevents dimerization and other follow reactions by blocking access to the re-

EurJIC
European Journal of Inorganic Chemistry

Full Paper
doi.org/10.1002/ejic.202000071

**Chemistry
Europe**
European Chemical
Societies Publishing

Table 1. Electrochemistry data for the investigated rhodocenium salts.[a]

	$E_{1/2}^{+/0}$ [V] (ΔE_p [mV])	$E_p^{0/-}$ [V][b] (ΔE_p [mV])	ΔE [V][c]	$E_{1/2}^{ox}$ [V][d] (ΔE_p [mV])
4-Me	−1.830 (88)	−2.820	−0.990	−0.72
7-SiMe$_3$	−1.765 (71)	−2.720	−0.955	−0.53
8-COOH	−1.535 (82)	n.a.[f]	n.a.[f]	−0.60
9[e]-COO$^-$	−1.900 (65)	n.a.[f]	n.a.[f]	−0.81
11-COOMe	−1.500 (91)	−2.615	−1.115	−0.51[e]
12-CONH$_2$	−1.645 (90)	−2.510	−0.865	−0.790
14[e]-NHCOMe	−1.715 (−)[f]	−2.230	−0.515	−0.800
Cp$_2$Rh$^{+[g]}$	−1.81 (−)	−2.58	−0.77	−0.90[f]
Cp*CpRh$^{+[h]}$	−2.07 (−)	−3.06	−0.99	−0.5[f]
Cp*$_2$Rh$^{+[h]}$	−2.38 (−)	−3.34	−0.96	n.a.
Cp′′′CpRh$^{+[i]}$	−1.83 (−)	n.a.	n.a.	n.a.
Cp′′′Cp*Rh$^{+[i]}$	−2.04 (−)	n.a.	n.a.	n.a.

[a] If not noted otherwise, data in dry, degassed THF/nBu$_4$PF$_6$ (0.1 M) under argon atmosphere, v = 0.1 V/s. Potentials are given on the ferrocene/ferrocenium scale ($E_{1/2}$ (Cp$_2$Fe$^{0/+}$) = 0.000 V). [b] Cathodic peak potential of an irreversible process. [c] Potential difference $E_{1/2}^{+/0}$ − $E_p^{0/-}$ between first and second reductions. [d] Peak potential of the anodic follow wave. [e] Data in DMF as solvent under otherwise identical conditions as in [a]. [f] No second reduction was observed within the available potential range. [g] Data in CH$_3$CN from ref.[11a,15] [h] Data in THF from ref.[12,15] [i] Data in THF from ref.[14b]

active sites, while the indenyl ligand of the latter complex can adapt to the decreasing electron demand of the rhodium ion by a hapticity change from η^5 to η^3. Such ring-slippage is particularly facile for indenyl ligands.[16]
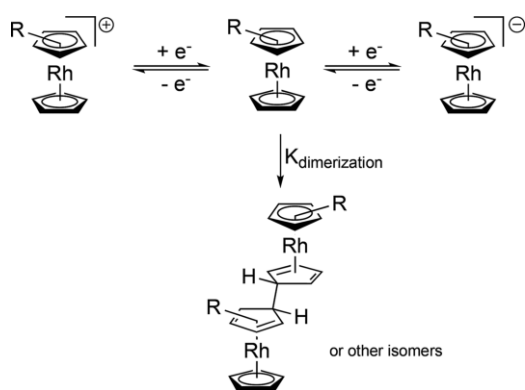
Scheme 2. The reduction of rhodocenium ions.

All of the above studies focused on rhodocenium ions with multiply substituted Cp rings. The present series of complexes provides us with the opportunity to probe the impact of a single ring substituent on the redox potential of a rhodocenium ion and the rate constant for dimerization following their initial one-electron reduction. Cyclic and square wave voltammograms of the various rhodocenium derivatives were measured in THF/NBu$_4$PF$_6$ and DMF/NBu$_4$PF$_6$ as the supporting electrolytes. In most cases the THF-based electrolyte produced somewhat better results in terms of the accessible potential range and the degree of chemical reversibility. Only in the cases of the N-acetylamide derivative **14** and of carboxylate **9** strong adsorption of the complex to the working electrode led to distortions of the reduction wave or additional features, which were absent in DMF.

Figure 8. compares representative cyclic voltammograms of the various rhodocenium derivatives at a sweep rate v of 0.1 V/s in THF (or, for **9** and **14** in DMF) at r. t.; relevant data are collected in Table 1. Voltammograms in DMF are shown as Figures S33 to S41 in the Supporting Information. All rhodocenium derivatives display a well-defined, chemically only par-

tially reversible wave or, in the case of amide derivative **12**, an irreversible cathodic peak, whose potential corresponds with the electronic properties of the respective substituent. Reduction potentials thus follow the ordering COOCH$_3$ ≈ COOH > CONH$_2$ > NHCOMe > SiMe$_3$ > Me > COO$^-$, in good qualitative match with the substituents' Hammett parameters.[17] For most derivatives, a second, completely irreversible reduction with an appreciably smaller peak height as compared to that of the +/0 couple was also observed. This decrease in peak height is due to competing dimerization of the rhodocene produced during the first reduction at the working electrode.
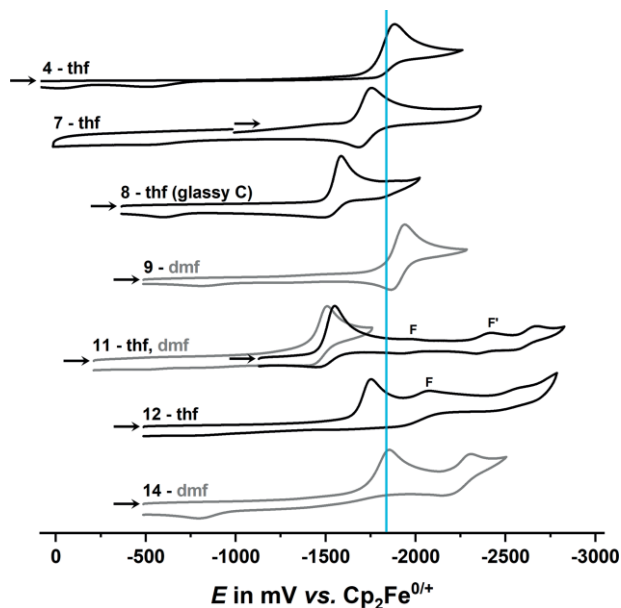
Figure 8. Cyclic voltammograms of the rhodocenium salts on a Pt working electrode (except for **8**, see text) in either DMF/nBu$_4$PF$_6$ (0.1 M) or THF/nBu$_4$PF$_6$ (0.1 M) at v = 0.1 V/s and at r.t. F and F′ denote small additional peaks/waves that most likely result from reduction at the rhodocenium substituent.

In principle, a smaller peak current for the second reduction peak would also be in line with the reduction of other electroactive follow product(s) formed by the corresponding rhodo-

EurJIC
European Journal of Inorganic Chemistry

Full Paper
doi.org/10.1002/ejic.202000071

Chemistry
Europe
European Chemical
Societies Publishing

cene. The assignment of this peak to the second reduction of the respective rhodocenium ion is therefore only tentative but in line with the potential separations of 770 to 990 mV for the two consecutive reductions observed for other rhodocenium ions (Table 1). In fact, additional features that are obviously due to other follow products formed after the first reduction are observed (marked as peaks F/F′ in Figure 8) in the case of derivatives **11** and **12**, which feature a reducible ester or amide substituent at the Cp ring.

The first, only partially reversible reduction gives also rise to one or two anodic follow peaks, which are solely observed after sweeping past the +/0 wave. In keeping with the well-established, general sequence of reaction steps in rhodocenium electrochemistry of Scheme 2, we assign this peak/these peaks to the oxidation of a neutral dihydrofulvalene-bridged dirhodium complex formed by dimerization of the 19 VE rhodocene. Peak potentials for this process are also provided in Table 1. The observation of two such peaks in the case of **4** probably indicates that two different isomers of this dimer are formed that are distinguished by which of the two different Cp rings couple in the C–C bond forming process. Such a situation was already reported for the mixed iridocene [Cp*CpIr].[18]

To further probe the dimerization hypothesis, we measured the concentration dependence and the peak current ratios for the first reduction wave and the first and second anodic counter peak for the methylrhodocenium ion **4**. A clear increase of the relative peak heights of the anodic follow peaks assignable to the oxidation of a dimer with increasing concentration levels was noted. This is in line with a higher order reaction involving the electrogenerated reduction product (Figure S42 of the Supporting Information). Thus, the ratio $i_{pa,fp}/i_{pc}$ for the first anodic peak (fp) increases from 0.023 to 0.109 on a fourfold increase of the initial concentration (Table 2). Moreover, the ratios of the peak currents of the two anodic follow peaks proved to be invariant to concentration within the experimental error limits, indicating that the underlying species most probably form in a parallel process. In general, the potential shifts of the +/0 wave of the monosubstituted rhodocenium ions with respect to the parent rhodocenium ion match qualitatively well with those reported for the 0/+ couple of the corresponding ferrocenes.[19] Table S38 of the Supporting Information provides such a comparison.

Table 2. Peak currents i_p for the reduction (i_{pc}) of **4** and the first and second anodic oxidation peaks of the follow products ($i_{pa,fp1}$, $i_{pa,fp2}$) from concentration-dependent cyclic voltammograms in THF at r.t.[a]

c [mM]	i_{pc} [μA]	$i_{pa,fp,1}$ [μA]	$i_{pa,fp,2}$ [μA]	$i_{pa,fp1}/i_{pc}$
6.4	43	4.7	4.2	0.109
4.4	30	2.5	3.0	0.083
3.4	23	1.7	1.6	0.074
1.6	11	0.3	0.3	0.023

[a] Data was recorded in dry, degassed THF with nBu$_4$PF$_6$ (40 mM) under argon atmosphere, v = 0.1 V/s.

There is, however, one notable exception, namely carboxylic acid **8**, when measured at a platinum or a gold working electrode. Based on the comparison of the half-wave potentials for the first oxidation of ferrocene carboxylic acid ($E_{1/2}^{0/+}$ = 0.19 V)

and of its methyl ester derivative ($E_{1/2}^{0/+}$ = 0.24 V, both in CH$_3$CN/NBu$_4$PF$_6$)[20] and on the differences of half-wave potentials between the free carboxylic acid and its deprotonated form, ferrocenecarboxylate, of 220 mV (CH$_3$CN/H$_2$O, 4:1[21] to 293 mV in the aprotic solvent PhCN,[22] one would expect that the first reduction of rhodocenium carboxylic acid **8** occurs at ca. –1.55 to –1.60 V. Instead, an unusually broad reduction peak at –1.235 V (THF) or –1.260 V (DMF) is observed as a chemically partially reversible (THF) or irreversible (DMF) process with a large potential splitting between the cathodic forward and the anodic return peak. The initial reduction of **8** produces another considerably more ideal (in an electrochemical, i.e. kinetic, sense), chemically partially reversible reduction feature, whose potential matches within experimental error that of the zwitterionic carboxylate derivative **9**. The reduction of rhodocenium carboxylic acid thus seems to follow a different pathway in that the COOH proton is reduced rather than the rhodocenium core, thus generating carboxylate **9** and molecular hydrogen [Equation (1)].

$$[CpRh(\eta^5\text{-}C_5H_4\text{-}COOH)]^+ + e^- \rightarrow [CpRh(\eta^5\text{-}C_5H_4\text{-}COO)] + 1/2\ H_2 \qquad (1)$$
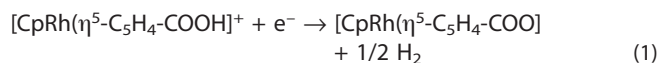
In order to further probe this hypothesis, we investigated the behavior of **8** at different working electrodes (note that reduction overpotentials for proton reduction depend on the electrode material) and in the presence of various amounts of tetramethylpiperidine as a strong, redox non-innocent and non-nucleophilic base. In the case of a metallocene-based reduction, the base would simply serve to alter the ratio of the free acid and its conjugate base, and hence the relative heights of the corresponding peaks/waves of these compounds, just as it was observed in the ferrocene case.[21] In the event of proton reduction, however, increasing the pH will strongly diminish the proton activity $a(H^+)$ and therefore induce sizeable cathodic shifts of the corresponding reduction peak. Both these anticipated effects were experimentally observed. Thus, the position of the first reduction wave differs strongly on Pt and Au working electrodes (Table 3), while that of the second one, which is assigned to the reduction of the associated carboxylate **9**, varies very little. Moreover, the proton reduction peak is completely absent at a glassy carbon electrode (see Figure 9, left; for square wave voltammograms see Figure S43 of the Supporting Information). Furthermore, incremental addition of tetramethylpiperidine base caused strong cathodic shifts of the broad reduction peak (Figure 9, right).

Table 3. Cyclic voltammetric experiments of the reduction of carbonic acid **8**.

Electrode material	$E_{p,f}$ [mV][a]	$E_{1/2}^{+/0}$ [mV] in DMF[b]
Pt	–1300	–1900
Au	–1555	–1870
Glassy C	–1535	–
Platinum (**9**)	–	–1900
Pt (**8**+0.1 eq of tmp)	–1730	–1900
Pt (**8**+0.2 eq of tmp)	–1790	–1900

[a] Peak potential for proton reduction. [b] Half-wave potential of the follow wave assigned to the reduction of zwitterionic carboxylate **9**.

In order to elucidate the substituent's effect on the dimerization rate, we estimated the dimerization rate constant k_{dim} by
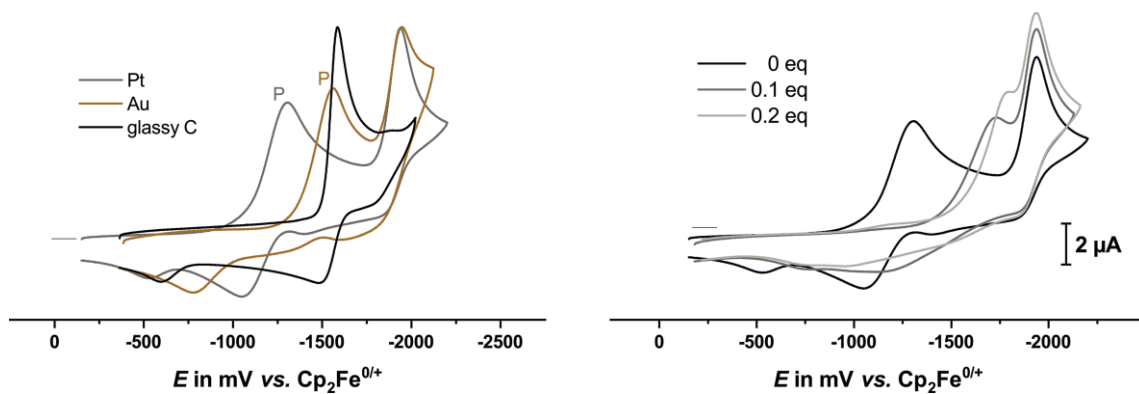
EurJIC
European Journal of Inorganic Chemistry

Full Paper
doi.org/10.1002/ejic.202000071

Chemistry
Europe
European Chemical
Societies Publishing

Figure 9. Left: cyclic voltammograms of **8** in DMF/nBu_4PF_6 at v = 0.1 V/s at r.t with a platinum (Pt), a gold (Au), or a glassy carbon (glassy C) electrode. Right: voltammograms with a platinum electrode in the presence of 0, 0.1 or 0.2 equivalents of 2,2,6,6-tetramethylpiperidine base.

digitally simulating voltammograms of every complex. Figures S48 to S54 of the Supporting Information provide exemplary comparisons between experimental and digitally computed voltammograms. The derived rate constants k_f and k_b as well as the equilibrium constant $K = k_f/k_b$ are provided in Table S39 of the Supporting Information. The forward rate constants for the rhodocene dimerization spread over two orders of magnitude and range from ca. 2×10^3 to 2.5×10^5 with an ordering CH_3, NH(C=O)Me < $SiMe_3$, C(=O)NH_2 < COOH, COO$^-$, COOMe. In particular, there are rather minor differences between the free carboxylic acid **8** and the corresponding carboxylate **9** in spite of the vastly different Hammett parameters of these two substituents and Coulombic repulsion between the two negatively charged monomers of reduced **9** as opposed to neutral rhodocene **8.**

Conclusions

A first chemoselective synthesis of rhodocenium carboxylic acid hexafluoridophosphate (**8**) has been developed via half-sandwich Rh(III) halide precursors. Common carboxylic acid derivatives like esters and amides are easily prepared, opening thereby new opportunities in bioorganometallic chemistry, e.g. peptide conjugates containing rhodocenium moieties, or in macromolecular and dendrimer chemistry, e.g. redox responsive polymers or dendrimers with rhodocenium groups. Unfortunately, aminorhodocenium is not yet accessible via Curtius rearrangement of the corresponding rhodocenium carboxylic azide, due to difficulties in separation of the various rhodocenium species formed. Spectroscopic and structural characterization of these first monosubstituted rhodocenium salts comprises $^1H/^{13}C$-NMR, IR, HR-MS and single crystal structure analyses on several derivatives. Attempted ^{103}Rh-NMR measurements of these monosubstituted rhodocenium salts met so far with limited success, due to the unfavorable magnetic properties of the ^{103}Rh nucleus. Like the parent rhodocenium ion and other substituted congeners, all new monosubstituted rhodocenium ions can be reduced to reactive rhodocenes. The reduction potentials follow the electronic substituent parameters of the corresponding substituent and shift to more negative (cathodic) values for stronger donors. The corresponding rhodocenes un-

dergo a rapid ($k = 2 \times 10^3$ s^{-1} to 2.5×10^5 s^{-1} as estimated from digital simulations of the cyclic voltammograms) chemical follow reaction, which competes with the second reduction process to the corresponding, even more reactive rhodocene anions. In agreement with an underlying dimerization process as it was established for other rhodocenes, the chemical reversibility of the first reduction decreases with increasing concentration of the analyte as was exemplarily shown for the methyl derivative **4**. Rhodocene carboxylic acid hexafluoridophosphate (**8**) constitutes a special case as it preferably undergoes reduction of the acidic COOH proton to generate zwitterionic rhodoceniumcarboxylate **9** plus dihydrogen at Pt or Au electrodes, but rhodocenium reduction on glassy carbon, where the overpotential for proton reduction is sufficiently large.

Experimental Section

General procedures: Synthetic work and spectroscopic characterization methods, including X-ray crystallography, were performed as recently described.[23] ^{103}Rh NMR spectra were measured at the University of Oslo on a Bruker BBO 500 MHz S2 10 mm (BBLR-H-D) with Z-gradient spectrometer. Starting materials were obtained commercially and used as received.

Electrochemical Measurements: All voltammetric measurements were conducted in a custom-made one-compartment cell with a spiral-shaped Pt wire and an Ag wire as the counter and reference electrodes respectively. As working electrode, a platinum (gold, glassy-carbon) electrode is used, that is polished with 1 μm and 0.25 μm diamond paste from Buehler-Wirtz consecutively prior to measurement. The cell is attachable to a conventional Schlenk line and all experiments were conducted under Argon atmosphere. The supporting electrolyte $NBu_4^+PF_6^-$ was dissolved in THF or DMF respectively to yield 5 mL of degassed analyte solution. Voltammograms were referenced by the addition of an internal reference of ferrocene. The data was acquired with a computer-controlled BASi potentiostat. Any additives were added to the cell under Argon (eg. 2,2,6,6-tetramethylpiperidine as a base). All simulations of cyclic voltammograms were conducted by using DigiSim[24] with the following fixed parameters: electrode surface area = 0.0256 cm^2, T = 298 K and non-Faradaic currents = 3.2×10^{-7} F and other variable parameters shown in Table S38 of the Supporting Information. Iteration of experimental cyclic voltammograms recorded over a scan rate range of 400–2000 mV/s, the program adjusted these variable

EurJIC
European Journal of Inorganic Chemistry

Full Paper
doi.org/10.1002/ejic.202000071

Chemistry
Europe
European Chemical
Societies Publishing

parameters to best universal fits of the CV shapes at any given scan rate.

Di(methylcyclopentadienyl)dirhodium(III) tetraiodide (3): Methyl-cyclopentadienide thallium (Cp′Tl) was prepared by reaction of 0.94 mL (9.33 mmol, 2.1 equiv.) of freshly cracked methylcyclopentadiene with 2.46 g (9.33 mmol, 2.1 equiv.) of TlOAc and 0.52 g (9.33 mmol, 2.1 equiv.) KOH in anhydrous ethanol under Ar-atmosphere. A white precipitate was formed and the reaction was carried on for one hour. Volatiles were removed in vacuo, the residue was dispersed in anhydrous THF, 2.19 g (4.44 mmol, 1 equiv.) of chlorido(cyclooctadiene)rhodium(I) dimer, [(cod)RhCl]$_2$ (**1**), was added and the reaction mixture was stirred for 3 hours. Workup under ambient conditions without protection from air: Volatiles were removed on a rotary evaporator, the residue was extracted with pentanes and, after removal of pentane on a rotary evaporator, yellow, oily (cyclooctadiene)(methylcyclopentadienyl)Rh(I) (**2**) was obtained. Without further purification and without protection from air, **2** was dissolved in dichloromethane and iodine (2.25 g, 8.88 mmol, 2 equiv.) was added. After 18 hours of stirring, heptane was added to the solution/dispersion, the dichloromethane was evaporated on a rotary evaporator, the precipitated product was filtered off on a fine glass frit, washed with pentane and dried in vacuo, affording 3.45 g (3.96 mmol, 89 %) of [Cp′RhI$_2$]$_2$ (**3**) as a dark brown powder. ^{1}H-NMR (300 MHz, CD$_2$Cl$_2$): δ = 2.23 (s, 3H, CH$_3$), 5.45 (d, 4H, ^{2}J(^{1}H-^{103}Rh) = 1.32 Hz, CpH) ppm. ^{13}C{^{1}H}-NMR (75 MHz, CD$_2$Cl$_2$): δ = 13.77 (CH$_3$), 83.4 (Cp), 85.7 (Cp) ppm. Single crystal structure analysis: Figure 2, supporting information.

Methylrhodocenium hexafluoridophosphate (4): A Schlenk vessel was charged under an atmosphere of Ar with 3.45 g (3.96 mmol, 1 equiv.) **3** and 50 mL of dry dichloromethane. To the resulting mixture 4.2 mL (8.32 mmol, 2.1 equiv.) of sodium cyclopentadienide solution in THF was added under vigorous stirring. A greyish precipitate formed, and the suspension was stirred overnight. Workup under ambient conditions: The mixture was filtered, water was added, and the dichloromethane was evaporated. The aqueous solution was filtered again, and the product was precipitated by addition of aqueous hexafluorophosphoric acid (1.23 mL, 8.32 mmol, 2.1 equiv.). The precipitate was filtered off, washed with cold water and dried in vacuo affording 2.39 g (6.1 mmol, 77 %) **4** as a white powder. If the product is still colored from residual iodine, the product can be purified by dissolving it in a saturated aqueous solution of sodium thiosulfate, then evaporating the water on a rotary evaporator and extracting the residue with acetone, filtering, evaporating the acetone and drying the now white product in vacuo. M.p: 280 °C (darkening/decomp. from 230 °C). ^{1}H-NMR (300 MHz, [D$_6$]acetone): δ = 2.25 (s, 3H, CH$_3$), 5.92 (br s, 2H, 2,5-Cp′), 6.03 (d, 5H, ^{2}J(^{1}H-^{103}Rh) = 0.9 Hz, Cp), 6.06 (br s, 2H, 3,4-Cp′) ppm. ^{13}C{^{1}H}-NMR (75 MHz, [D$_6$]acetone): δ = 13.77 (s, CH$_3$), 86.90 (d, ^{1}J(^{13}C-^{103}Rh) = 7.15 Hz, 2,5-Cp′), 88.29 (d, ^{1}J(^{13}C-^{103}Rh) = 6.86 Hz, 3,4-Cp′ and Cp), 108.39 (d, ^{1}J(^{13}C-^{103}Rh) = 6.9 Hz, 1-Cp′) ppm. MS (MALDI pos): C$_{11}$H$_9$RhPF$_6$, calcd. most abundant isotope peak m/z = 246.9994 (M – PF$_6$)$^+$, found m/z = 247.0055. IR (ATR): $\tilde{v}$ = 3128 (w, v_{C-H}), 1477 (w), 1454 (w), 1417 (w), 1396 (w), 1378 (w), 1033 (w), 1009 (w), 900 (w), 878 (w), 810 (s, v_{P-F}), 628 (w), 553 (s, v_{P-F}), 413 (m) cm^{-1}.

Di(trimethylsilylcyclopentadienyl)dirhodium(III) tetraiodide (6): A Schlenk vessel was charged with trimethylsilylcyclopentadiene (69.0 µL, 0.42 mmol, 2.1 equiv.) and 15 mL of anhydrous THF. The mixture was cooled to –80 °C and 168 µL of a 2.5 M butyllithium hexane solution (0.42 mmol, 2.1 equiv.) was added to effect deprotonation. The solution was warmed to approximately 0 °C and chlorido(cyclooctadiene)rhodium(I) dimer, [(cod)RhCl]$_2$ (**1**) (97.6 mg, 0.20 mmol) was added. After stirring for two hours the solvent was

evaporated, the residue extracted with pentane, filtered and the solvent was evaporated, affording a yellow oil of (cyclooctadiene)-(trimethylsilylcyclopentadienyl)Rh(I) (**5**). Without protection from air, this material was dissolved in dichloromethane and iodine (101.5 mg, 0.40 mmol, 2.0 equiv.) was added. After stirring overnight, heptane was added, dichloromethane was evaporated and the product was filtered off, washed with pentane and dried in vacuo, affording 149.6 mg (0.15 mmol, 76.2 yield%) **6**. ^{1}H-NMR (300 MHz, CD$_2$Cl$_2$): δ = 0.36 (s, 9H, TMS), 5.59 (m, 2H, Cp), 5.66 (m, 2H, Cp) ppm. ^{13}C{^{1}H}-NMR (75 MHz, CD$_2$Cl$_2$): δ = 0.26 (s, TMS), 85.61 (d, ^{1}J(^{13}C-^{103}Rh) = 6.79 Hz, Cp), 86.39 (d, ^{1}J(^{13}C-^{103}Rh) = 6.81 Hz, Cp), 92.20 (d, ^{1}J(^{13}C-^{103}Rh) = 6.46 Hz, Cp) ppm.

Trimethylsilylrhodocenium hexafluoridophosphate (7): A Schlenk vessel was charged with **6** (149.6 mg, 0.15 mmol, 1 equiv.) and 10 mL of anhydrous acetone. AgPF$_6$ (80.6 mg, 0.32 mmol, 2.1 equiv.) was added and the mixture was stirred under protection from light for one hour, resulting in red suspension. Thallium cyclopentadienide (89.6 mg, 0.33 mmol, 2.2 equiv.) was added and the mixture was stirred overnight. Then the solution was concentrated to about a tenth of its volume and diethyl ether was added. Solids were filtered off and washed with acetone/ether (v:v = 1:5). The solvents were evaporated, and the residue dried in vacuo to yield 118.3 mg of **7** (0.26 mmol, 87 %) as a greyish crystalline powder. M.p: 250 °C (decomp.). ^{1}H-NMR (300 MHz, CD$_2$Cl$_2$): δ = 0.30 (s, 9H, TMS), 5.77 (m, 2H, Cp^{TMS}), 5.86 (d, ^{2}J(^{1}H-^{103}Rh) = 0.97 Hz, 5H, Cp), 6.01 (m, 2H, Cp^{TMS}) ppm. ^{13}C{^{1}H}-NMR (75 MHz, CD$_2$Cl$_2$): δ = 0.45 (s, TMS), 87.52 (d, ^{1}J(^{13}C-^{103}Rh) = 6.78 Hz, Cp), 89.77 (d, ^{1}J(^{13}C-^{103}Rh) = 7.31 Hz, Cp^{TMS}), 91.70 (d, ^{1}J(^{13}C-^{103}Rh) = 7.20 Hz, Cp^{TMS}) ppm. MS (FTMS + pESI Full MS): C$_{13}$H$_{18}$SiRhPF$_6$, calcd. most abundant isotope peak m/z = 305.0233 (M – PF$_6$)$^+$, found m/z = 305.0217. IR (ATR): $\tilde{v}$ = 3124 (w, v_{C-H}), 2960 (w), 1417 (m), 1388 (m), 1259 (m), 1248 (m), 1160 (m), 1043 (m), 1011 (w), 897 (m), 883 (m), 818 (s, v_{P-F}), 761 (s), 701 (w), 629 (m), 555 (s, v_{P-F}), 461 (m), 428 (m) cm^{-1}. Single crystal structure analysis: Figure 3, supporting information.

Rhodoceniumcarboxylic acid hexafluoridophosphate (8): A solution of **4** (2.39 g, 6.1 mmol, 1 equiv.), KMnO$_4$ (2.41 g, 6.1 mmol, 2.5 equiv.) and 1.83 mL (18.3 mmol, 3 equiv.) 10 M NaOH in water was refluxed for 18 h. After cooling to room temperature, MnO$_2$ was filtered off and washed with five portions of acetonitrile. After the organic fractions were evaporated and the remaining aqueous solution was concentrated on a rotary evaporator, 4.5 mL (27.5 mmol, 4.5 equiv.) aqueous HPF$_6$ was then added at 0 °C. The white precipitate was filtered off and washed with cold water. The product (2.32 g, 5.5 mmol, 90.0 %) was dissolved in acetone and filtered, the solution was concentrated, and the white powder dried in vacuo. If traces of methylrhodocenium (from incomplete oxidation) or rhodocenium (from cyclopentadiene-containing methylcyclopentadiene) are found, recrystallization from an acetone/dichloromethane/diethyl ether (4:2:1) mixture afforded rhodeniumcarboxylic acid hexafluorophosphate (**8**). Crystals suitable for X-ray analysis were obtained by slow evaporation of a solution in acetone. M.p: 240–250 °C (decomp.). ^{1}H-NMR (300 MHz, CD$_3$CN): δ = 5.93 (d, 5H, ^{2}J(^{1}H-^{103}Rh) = 0.75 Hz, Cp), 5.96 (m, 2H, 3,4-Cp^{COOH}), 6.27 (m, 2H, 2,5- Cp^{COOH}) ppm. ^{13}C{^{1}H}-NMR (75 MHz, CD$_3$CN): δ = 89.02 (d, ^{1}J(^{13}C-^{103}Rh) = 6.80 Hz, 3,4- Cp^{COOH}), 89.44 (d, ^{1}J(^{13}C-^{103}Rh) = 6.99 Hz, Cp), 90.16 (d, ^{1}J(^{13}C-^{103}Rh) = 6.76 Hz, 2,5-Cp^{COOH}), 93.77 (d, J = 8.75 Hz, 1-Cp^{COOH}), 163.76 (s, COOH) ppm. MS (MALDI pos, [m/z]): C$_{11}$H$_{10}$O$_2$RhPF$_6$, calcd. most abundant isotope peak m/z = 276.9736 (M – PF$_6$)$^+$, found m/z = 277.0050. IR (ATR): $\tilde{v}$ = 3129 (w, v_{C-H}), 1709 (m, $v_{C=O}$), 1584 (w), 1491 (m), 1415 (m), 1298 (m), 1178 (m), 1031 (m), 807 (s, v_{P-F}), 751 (s), 553 (s, v_{P-F}), 454 (m) cm^{-1}. Single crystal structure analysis: Figure 4, supporting information.

EurJIC
European Journal of Inorganic Chemistry

Full Paper
doi.org/10.1002/ejic.202000071

Chemistry
Europe
European Chemical
Societies Publishing

Rhodoceniumcarboxylate (9): A concentrated solution of **8** (280 mg, 0.60 mmol) in 8 mL of water/acetonitrile, 3:1 was poured upon a column filled with DOWEX Marathon A™ anion-exchange resin and slowly eluted. After evaporating of solvents the yellowish product was dried in vacuo, it is slightly hygroscopic. Yield: 93 % (153 mg, 0.55 mmol). M.p. 240 °C (decomp.). ^{1}H-NMR (300 MHz, [D$_4$]methanol): δ = 5.97 (m, 2H, Cp^{COO-}), 5.99 (d, ^{2}J(^{1}H-^{103}Rh) = 0.97 Hz, 5H, Cp), 6.22 (m, 2H, Cp^{COO-}) ppm. ^{13}C{^{1}H}-NMR (75 MHz, [D$_4$]methanol): δ = 88.80 (d, ^{1}J(^{13}C-^{103}Rh) = 2.55 Hz, Cp^{COO-}), 88.89 (d, ^{1}J(^{13}C-^{103}Rh) = 2.85 Hz, Cp^{COO-}), 88.98 (d, ^{1}J(^{13}C-^{103}Rh) = 7.08 Hz, Cp) ppm. IR (ATR): $\tilde{v}$ = 3367 (broad, m), 3099 (m), 3068 (m), 1598 (s), 1455 (m), 1415 (m), 1398 (m), 1382 (m), 1356 (m), 1331 (m), 1029 (m), 1006 (m), 897 (m), 857 (m), 807 (m), 777 (m), 699 (m), 576 (m), 530 (m), 452 (m) cm^{-1}.

Rhodoceniumcarboxylic acid chloride hexafluoridophosphate (10): Rhodoceniumcarboxylic acid hexafluoridophosphate (**5**) (380 mg, 0.900 mmol) was refluxed in 13 mL of thionyl chloride overnight. The excess of thionyl chloride was then evaporated and the residue dried in vacuo. The slightly orange, air-sensitive powder was then used directly for further reactions. IR (ATR): $\tilde{v}$ = 3126 (w, v_{C-H}), 1768 (m, $v_{C=O}$), 1718 (m), 1416 (w), 1401 (w), 1236 (m), 1049 (m), 942 (w), 823 (s), 790 (s, v_{P-F}), 554 (s, v_{P-F}), 452 (m), 409 (m) cm^{-1}.

Methoxycarbonylrhodocenium hexafluoridophosphate (11): Rhodoceniumcarboxylic acid hexafluoridophosphate (**5**) (100.2 mg, 0.237 mmol) was transformed to the acid chloride as described above, dried and dissolved in 5 mL of dry methanol. After stirring overnight and evaporating to dryness the residue was extracted with acetone, the solution filtered, evaporated to dryness and the product dried in vacuo. Crystals suitable for X-ray analysis were obtained by slow evaporation of a solution in methanol. Yield: 65.6 % (67.9 mg, 0.156 mmol). M.p. 225 °C (decomp.). ^{1}H-NMR (300 MHz, [D$_6$]acetone): δ = 3.87 (s, 3H, OCH$_3$), 6.23 (d, 5H, ^{2}J(^{1}H-^{103}Rh) = 0.9 Hz, Cp), 6.26 (m, 2H, Cp'), 6.53 (m, 2H, Cp') ppm. ^{13}C{^{1}H}-NMR (75 MHz, [D$_6$]acetone): δ = 53.63 (s, OCH$_3$), 88.87 (d, ^{1}J(^{13}C-^{103}Rh) = 6.65 Hz, Cp^{COOMe}), 89.51 (d, ^{1}J(^{13}C-^{103}Rh) = 7.41 Hz, Cp), 90.26 (d, ^{1}J(^{13}C-^{103}Rh) = 7.03 Hz, Cp^{COOMe}) ppm. MS (FTMS + pESI Full MS): C$_{12}$H$_{12}$O$_2$RhPF$_6$, calcd. most abundant isotope peak m/z = 290.9892 (M – PF$_6$)$^+$, found m/z = 290.9879. IR (ATR): $\tilde{v}$ = 3115 (m, v_{C-H}), 2953 (w), 1721 (s, $v_{C=O}$), 1473 (m), 1416 (m), 1397 (w), 1285 (m), 1153 (m), 1031 (m), 1008 (m), 964 (m), 900 (w), 822 (s, v_{P-F}), 777 (s), 554 (s, v_{P-F}), 498 (m), 453 (m) cm^{-1}. Single crystal structure analysis: Figure 5, supporting information.

Rhodoceniumcarboxylic acid amide hexafluoridophosphate (12): Rhodoceniumcarboxylic acid chloride hexafluoridophosphate (**10**) (from 601 mg, 1.42 mmol rhodocenium carboxylic acid hexafluoridophosphate (**8**)) was dissolved in 10 mL of dry acetonitrile and 0.53 mL (7.12 mmol, 5 equiv.) of 25 % ammonia in water was added. The solution was stirred for two hours, filtered and the solvents evaporated to dryness. Drying in vacuo yielded 57 % (344 mg, 0.817 mmol) **12** as slightly greyish crystalline powder. Single crystals suitable for X-ray analysis were grown by slow concentration of a solution in acetonitrile. M.p. 173 °C. ^{1}H-NMR (300 MHz, CD$_3$CN): δ = 5.90 (d, ^{2}J(^{1}H-^{103}Rh) = 1.00 Hz, 5H, Cp), 5.91 (m, 2H, 2,5-Cp^{CONH2}), 6.25 (m, 2H, 3,4- Cp^{CONH2}), 6.73 (br s, 2H, NH$_2$) ppm. ^{13}C{^{1}H}-NMR (75 MHz, CD$_3$CN): δ = 88.00 (d, ^{1}J(^{13}C-^{103}Rh) = 6.93 Hz, 2,5-Cp^{CONH2}), 89.59 (m, Cp and 3,4- Cp^{CONH2}), 163.52 (s, CONH$_2$) ppm. MS (MALDI pos): C$_{11}$H$_{11}$NORhPF$_6$, calcd. most abundant isotope peak m/z = 275.9896 (M – PF$_6$)$^+$, found m/z = 275.9996. IR (ATR): $\tilde{v}$ = 3460 (w), 3315 (w), 3128 (w, v_{C-H}), 2923 (w), 2853 (w), 1687 (m, amide I), 1618 (w, amid II), 1474 (w), 1419 (m), 1396 (m), 1334 (w), 1249 (w), 1175 (w), 1137 (w), 1071 (w), 1029 (m), 955 (m), 904 (w), 809 (s, v_{P-F}), 778

(s), 686 (m), 642 (w), 598 (w), 553 (s, v_{P-F}), 523 (m), 442 (m) cm^{-1}. Single crystal structure analysis: Figure 6, supporting information.

Rhodoceniumcarboxylic acid azide hexafluoridophosphate (13): Rhodoceniumcarboxylic acid chloride hexafluoridophosphate (**10**) (from 380 mg, 0.900 mmol rhodocenium carboxylic acid hexafluoridophosphate (**8**)) was dissolved in a mixture of dry nitromethane and tBuOH (v/v = 1:1). Under stirring, NaN$_3$ (1.17 g, 18.0 mmol, 20 equiv.) was added and after 4 hours solvents were evaporated, the residue was extracted with acetone, filtered, the solvent was evaporated and the residue was dried in vacuo. Quantitative transformation is assumed, the azide is used immediately for further reactions. IR (ATR): $\tilde{v}$ = 3127 (w, v_{C-H}), 2201 (w), 2156 (w), 1688 (m, $v_{C=O}$), 1609 (w), 1462 (w), 1417 (w), 1398 (w), 1371 (w), 1265 (m), 1184 (m), 1054 (w), 1030 (w), 1003 (w), 899 (w), 810 (s, v_{P-F}), 751 (s), 639 (w), 554 (s, v_{P-F}), 490 (w), 434 (m), 407 (m) cm^{-1}.

Acetamidorhodocenium chloride hydrate (14): Freshly prepared rhodoceniumcarboxylic acid azide hexafluorophosphate (**13**) (from 380 mg, 0.900 mmol rhodoceniumcarboxylic acid hexafluorophosphate (**8**)) was dissolved in acetic acid anhydride and 240 mg (1.8 mmol, 2 equiv.) AlCl$_3$ was added. After reflux overnight 5 mL of water was slowly added under cooling and stirring for another 30 min. Then the solution was evaporated to dryness and extracted with acetonitrile, filtered, again evaporated to dryness and dried in vacuo, affording 174 mg of **14** (0.54 mmol, 60 %). Single crystals suitable for X-ray analysis were grown by slow concentration of a solution in methanol. M.p. 259 °C (loss of water from 120 °C). ^{1}H-NMR (300 MHz, [D$_4$]methanol): δ = 2.08 (s, 3H, CH$_3$), 5.80 (m, 2H, Cp'), 5.94 (d, 5H, ^{2}J(^{1}H-^{103}Rh) = 0.7 Hz, Cp), 6.32 (m, 2H, Cp') ppm. ^{13}C{^{1}H}-NMR (75 MHz, [D$_4$]methanol): δ = 23.63 (CH$_3$), 77.90 (d, ^{1}J(^{13}C-^{103}Rh) = 6.92 Hz, Cp^{NHR}), 83.69 (d, ^{1}J(^{13}C-^{103}Rh) = 8.64 Hz, Cp^{NHR}), 88.30 (d, ^{1}J(^{13}C-^{103}Rh) = 7.72 Hz, Cp) ppm. MS (FTMS + pESI Full MS): C$_{12}$H$_{13}$NORhPF$_6$, calcd. most abundant isotope peak m/z = 290.0052 (M – PF$_6$)$^+$, found m/z = 290.0035. IR (ATR): $\tilde{v}$ = 3481 (w), 3406 (w), 3151 (w), 3083 (w), 2991 (w), 2769 (w), 1719 (w), 1692 (m), 1609 (w), 1551 (m), 1490 (m), 1415 (w), 1390 (w), 1375 (m), 1336 (w), 1266 (m), 1245 (m), 1105 (w), 1042 (m), 1009 (m), 842 (m), 756 (w), 648 (w), 604 (w), 580 (w), 556 (w), 474 (w), 449 (w), 419 (m) cm^{-1}. Single crystal structure analysis: Figure 7, supporting information.

CCDC 1973357 (for **3**), 1973358 (for **7**), 1973359 (for **8**), 1973360 (for **11**), 1973361 (for **12**), and 1973362 (for **14**) contain the supplementary crystallographic data for this paper. These data can be obtained free of charge from The Cambridge Crystallographic Data Centre.

[1] a) S. Vanicek, H. Kopacka, K. Wurst, T. Müller, H. Schottenberger, B. Bildstein, *Organometallics* **2014**, *33*, 1152–1156; b) S. Vanicek, H. Kopacka, K. Wurst, T. Müller, C. Hassenrück, R. F. Winter, B. Bildstein, *Organometallics*

EurJIC
European Journal of Inorganic Chemistry

Full Paper
doi.org/10.1002/ejic.202000071

Chemistry Europe
European Chemical Societies Publishing

2016, *35*, 2101–2109; c) M. Jochriem, D. Bosch, H. Kopacka, B. Bildstein, *Organometallics* **2019**, *38*, 2278–2279.

[2] a) S. Vanicek, M. Jochriem, C. Hassenrück, S. Roy, H. Kopacka, K. Wurst, T. Müller, R. F. Winter, E. Reisner, B. Bildstein, *Organometallics* **2019**, *38*, 1361–1371; b) S. Vanicek, M. Podewitz, J. Stubbe, D. Schulze, H. Kopacka, K. Wurst, T. Müller, P. Lippmann, S. Haslinger, H. Schottenberger, K. R. Liedl, I. Ott, B. Sarkar, B. Bildstein, *Chem. Eur. J.* **2018**, *24*, 3742–3753; c) S. Vanicek, M. Podewitz, C. Hassenrück, M. Pittracher, H. Kopacka, K. Wurst, T. Müller, K. R. Liedl, R. F. Winter, B. Bildstein, *Chem. Eur. J.* **2018**, *24*, 3165–3169; d) S. Vanicek, H. Kopacka, K. Wurst, S. Vergeiner, S. Kankowski, J. Schur, B. Bildstein, I. Ott, *Dalton Trans.* **2016**, *45*, 1345–1348; e) S. Vanicek, H. Kopacka, K. Wurst, S. Vergeiner, L. Oehninger, I. Ott, B. Bildstein, *Z. Anorg. Allg. Chem.* **2015**, *641*, 1282–1292.

[3] *SciFinder© literature search*, September **2019** with search profile "rhodocenium, rhodicenium, rhodicinium": 47 publications, 3 monosubstituted compounds.

[4] J. E. Sheats, W. C. Spink, R. A. Nabinger, D. Nicol, G. Hlatky, *J. Organomet. Chem.* **1983**, *251*, 93–102.

[5] M. Andre, H. Schottenberger, R. Tessadri, G. Ingram, P. Jaitner, K. E. Schwarzhans, *Chromatographia* **1990**, *30*, 543–545.

[6] Y. Yan, T. M. Deaton, J. Zhang, H. He, J. Hayat, P. Pageni, K. Matyjaszewski, C. Tang, *Macromolecules* **2015**, *48*, 1644–1650.

[7] a) D. A. Loginov, M. M. Vinogradov, Z. A. Starikova, P. V. Petrovskii, A. R. Kudinov, *Russ. Chem. Bull.* **2004**, *53*, 1949–1953; b) X. You-Feng, S. Yan, P. Zhen, *J. Organomet. Chem.* **2004**, *689*, 823–832; c) M. A. Mantell, J. W. Kampf, M. Sanford, *Organometallics* **2017**, *36*, 4382–4393; d) W. Lin, W. Li, D. Lu, F. Su, T.-B. Wen, H.-J. Zhang, *ACS Catal.* **2018**, *8*, 8070–8076.

[8] D. A. Loginov, L. S. Shul'pina, D. V. Muratov, G. B. Shul'pin, *Coord. Chem. Rev.* **2019**, *387*, 1–31.

[9] a) H. Lebel, O. Leogane, *Org. Lett.* **2005**, *7*, 4107–4110; b) M. V. Zabalov, R. P. Tiger, *THEOCHEM* **2010**, *962*, 15–22.

[10] Reviews: a) M. A. Fedotov, *J. Struct. Chem.* **2016**, *57*, 563–613; b) J. M. Ernsting, S. Gaemers, C. J. Elsevier, *Magn. Reson. Chem.* **2004**, *42*, 721–736.

[11] a) N. El Murr, J. E. Sheats, W. E. Geiger Jr., J. D. L. Holloway, *Inorg. Chem.* **1979**, *18*, 1443–1446; b) K. Moudgil, M. A. Mann, C. Risko, L. A. Bottomley, S. R. Marder, S. Barlow, *Organometallics* **2015**, *34*, 3706–3712.

[12] O. V. Gusev, L. I. Denisovich, M. G. Peterleitner, A. Z. Rubezhov, N. A. Ustynyuk, P. M. Maitlis, *J. Organomet. Chem.* **1993**, *452*, 219–222.

[13] S. K. Mohapatra, A. Romanov, G. Angles, T. V. Timofeeva, S. Barlow, S. R. Marder, *J. Organomet. Chem.* **2012**, *706–707*, 140–143.

[14] a) B. T. Donovan-Merkert, H. I. Tjiong, L. M. Rhinehart, R. A. Russell, J. Malik, *Organometallics* **1997**, *16*, 819–821; b) B. T. Donovan-Merkert, C. R. Clontz, L. M. Rhinehart, H. I. Tjiong, C. M. Carlin, T. R. Cundari, A. L. Rheingold, I. Guzei, *Organometallics* **1998**, *17*, 1716–1724.

[15] J. E. Collins, M. P. Castellani, A. L. Rheingold, E. J. Miller, W. E. Geiger, A. L. Rieger, P. H. Rieger, *Organometallics* **1995**, *14*, 1232–1238.

[16] a) M. E. Rerek, L.-N. Ji, F. Basolo, *J. Chem. Soc., Chem. Commun.* **1983**, 1208–1209; b) J. M. O'Connor, C. P. Casey, *Chem. Rev.* **1987**, *87*, 307–318.

[17] C. Hansch, A. Leo, R. W. Taft, *Chem. Rev.* **1991**, *91*, 165–195.

[18] O. V. Gusev, M. G. Peterleitner, M. A. Ievlev, A. M. Kal'sin, P. V. Petrovskii, L. I. Denisovich, N. A. Ustynyuk, *J. Organomet. Chem.* **1997**, *531*, 95–100.

[19] a) W. F. Little, C. N. Reilley, J. D. Johnson, A. P. Sanders, *J. Am. Chem. Soc.* **1964**, *86*, 1382–1386; b) S. Lu, V. V. Strelets, M. F. Ryan, W. J. Pietro, A. B. P. Lever, *Inorg. Chem.* **1996**, *35*, 1013–1023; c) T. Kienz, C. Förster, K. Heinze, *Organometallics* **2014**, *33*, 4803–4812; d) C. P. Andrieux, A. Merz, J. M. Saveant, R. Tomahogh, *J. Am. Chem. Soc.* **1984**, *106*, 1957–1962; e) P. T. N. Nonjola, U. Siegert, J. C. Swarts, *J. Inorg. Organomet. Polym. Mater.* **2015**, *25*, 376–385.

[20] J. Podlaha, P. Štěpnička, J. Ludvík, I. Císařová, *Organometallics* **1996**, *15*, 543–550.

[21] G. De Santis, L. Fabbrizzi, M. Licchelli, P. Pallavicini, *Inorg. Chim. Acta* **1994**, *225*, 239–244.

[22] T. Honda, T. Nakanishi, K. Ohkubo, T. Kojima, S. Fukuzumi, *J. Am. Chem. Soc.* **2010**, *132*, 10155–10163.

[23] I. Schlapp-Hackl, C. Hassenrück, K. Wurst, H. Kopacka, T. Müller, R. F. Winter, B. Bildstein, *Eur. J. Inorg. Chem.* **2018**, 4434–4441.

[24] M. Rudolph, S. Feldberg, **1994**, DigiSim3, Version 3.03, Bioanalytical Systems, Inc. PK.